Vortex Interactions in Multiple Vortex Wakes behind Aircraft

Donald L. Ciffone*
NASA Ames Research Center, Moffett Field, Calif.

A flow visualization technique has been developed that allows the nature of lift-generated wakes behind aircraft models to be investigated. The technique is applicable to models being towed underwater in a ship model basin. Several different configurations of a 0.61-m (2-ft) span model of a Boeing 747-type transport aircraft were tested to allow observation of typical vortex interactions and merging in multiple vortex wakes. The vortices were identified by emitting tracer dyes from selected locations on the model. Their trajectories were obtained from photographs of the wake. Wingspan loading and model attitude were found to effect both vortex motions within the wake and resulting far-field wake velocity. Landing-gear deployment caused a far-field reformation of vorticity behind a model configuration which dissipated concentrated vorticity in the near-field wake. Circulation from the wing always caused a downward movement of the horizontal tail vortices, which merged with wing vortices. A modified landing configuration was developed that appeared to significantly alleviate the concentrated wake vorticity associated with the current landing configuration.

Nomenclature

b_e	= distance between centers of vorticity on each side of wing
b_{IF}	= inboard flap span
$\bar{c}$	= mean aerodynamic chord
$c(y)$	= local wing chord
C_{D_i}	= theoretically estimated induced drag coefficient
C_l	= section lift coefficient
CLEAN	= cruise configuration, no surfaces deflected
C_{L_T}	= theoretically estimated lift coefficient
D_F	= measured distance between vortices from the outboard edge of inboard flaps
D_{F_0}	= initial measurement of distance between inboard flap outer-edge vortices
D_L	= spacing between outboard flap outer-edge vortices
D_V	= measured vertical distance between highest position of wingtip vortex above wing and subsequent positions
D_W	= measured distance between wingtip vortices
D_{W_0}	= initial measurement of distance between wingtip vortices
LDG	= landing configuration, inboard and outboard flaps deflected 46 deg. leading-edge flaps deployed
LDG/O	= same as LDG but with outboard flaps retracted
MOD LDG	= same as LDG but with 30% of inboard span of inboard flap removed
MOD LDG/O	= same as LDG/O but with 30% of inboard span of inboard flap removed
MOD LDG/T.O.	= same as MOD LDG/O but with outboard flaps deflected 7 deg.
U_∞	= towing speed, m/sec
w	= vortex sink rate, cm/sec
X/b	= downstream distance in span lengths
$y/(b/2)$	= fraction semispan
α	= model angle of attack, deg

Received Jan. 12, 1976; presented as Paper 76-62 at the AIAA 14th Aerospace Sciences Meeting, Washington, D.C., Jan. 26-28, 1976; revision received Oct. 7, 1976.

Index categories: Aircraft Aerodynamics (including Component Aerodynamics); Aircraft Testing (including Component Wind-Tunnel Testing); Jets, Wakes, and Viscid-Inviscid Flow Interactions.

*Research Scientist. Associate Fellow AIAA.

Introduction

THEORETICAL studies[1,2] have indicated that by modifying the wingspan loading of an aircraft, the rotational velocities within its wake can be reduced significantly. The studies were verified in ground-based experiments both on the conceptual level[3] and in application to a Boeing 747-type transport model.[4,5] However, recent flight tests[6,7] have indicated that, although the span loading can be modified to substantially reduce wake rotational velocities, the deployment of landing gear and/or yawing motions of the aircraft can substantially reduce the benefits of span-load alterations. Subsequent wind-tunnel tests did not identify significant differences in wake geometry, velocity, or induced rolling moment on a following model due to deployment of landing gear of a wake-generating model. Consequently, it was decided to develop a flow-visualization technique to be used in a water tow tank (ship-model basin) to allow better understanding of the vortex interactions and merging characteristics in multiple vortex wakes. In particular, the tow tank was selected to allow the far-field wake to be examined for differences in wake vorticity as a result of landing-gear deployment.

The tests were performed in the University of California's water tow-tank facility at Richmond, California. In this method of testing, the model is towed underwater, generating a continuous wake that decays with time at each longitudinal point of the test gallery. The only restriction to test time comes from either the ultimate interference from walls or floor or the passage through the test section of internal vortex waves, which arise from starting or stopping the model at the beginning and end of the towing range. Previous tests in this facility allowed undisturbed measurements of wake velocities to 200 span lengths behind the mode.[3,8]

Comprehensive photographic results were obtained of the wake of a 0.01-scale model of a Boeing-747 transport with various wingspan loadings with landing gear both deployed and retracted. These results cover a large portion of the time history of vortex interactions typical of multiple-vortex wakes shed by transport-type aircraft. They will be used to update existing wake-vortex models and guide the development of future theoretical models.

Experimental Apparatus and Procedure

Facility and Model Description

The test facility was the University of California's water tow tank located in Richmond, California. The tank is 61 m long, 2.44 m wide, and 1.7 m deep. The model was towed past

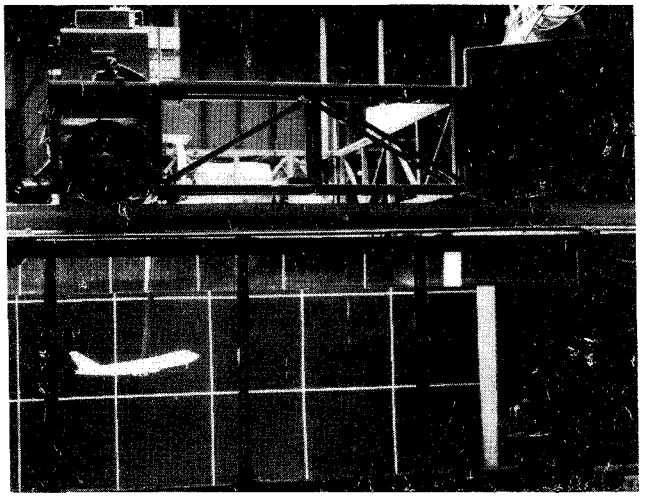

Fig. 1 Model installation photograph.

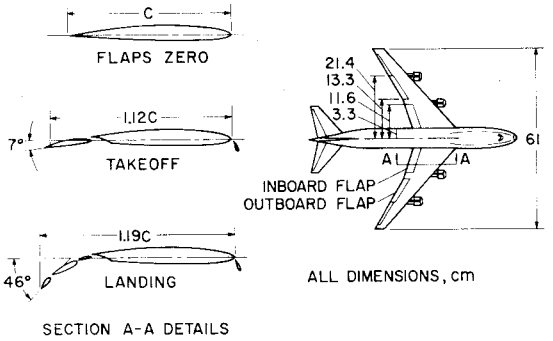

Fig. 2 0.01-scale model of Boeing-747 airplane.

a viewing station (Fig. 1) located approximately 14 m from the starting point of the carriage and 21 m from the stopping location. The mean chord Reynolds number at a towing speed of 2 m/sec was $1.64 \times 10.^5$ Principal geometric characteristics of the model are presented in Table 1.

The model is equipped with leading-edge flaps, triple-slotted trailing-edge flaps (Fig. 2), removable landing gear (Fig. 3), flow-through nacelles, and a variable incidence tail. Except for the CLEAN (cruise) configuration and where specifically noted in the paper, all of the model configurations were tested with the gear deployed.

Table 1 Principal geometric characteristics of B-747 0.01-scale model

Element	cm (in.)
Wing	
Span	61.0 (24.0)
Root incidence	2.0 deg
Tip incidence	−2.0 deg
Mean aerodynamic chord	8.71 (3.43)
Root chord	16.7 (6.57)
Tip chord	4.06 (1.6)
Sweepback (at 1/4 chord)	37.5 deg
Area, cm^2 (ft^2)	536.0 (0.578)
Aspect ratio	6.96
Fuselage	
Length	70.2 (27.6)
Horizontal stabilizer	
Span	22.6 (8.9)
Area, cm^2 (ft^2)	143.0 (0.154)
Aspect ratio	3.6

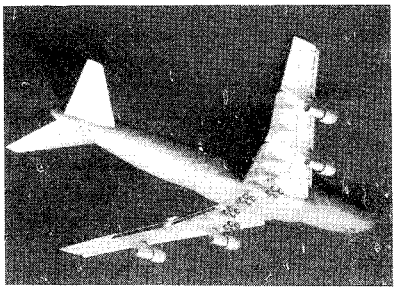

Fig. 3 Photograph of model in landing configuration; viewed from below and aft.

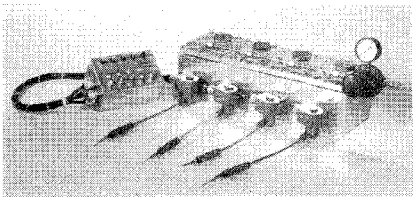

Fig. 4 Dye reservoir and ejection system.

Flow-Visualization Technique

To observe the vortices in the model's trailing wake, the model is equipped with dye-ejection orifices located at the wingtips, the outboard and inboard edges of the inboard flaps, and at the tips of the horizontal stabilizer. Manifolds and solenoid activated valves were used to release various combinations of dye from a pressurized reservoir (Fig. 4) to the model.

As the model passed through the viewing station, a cross section through its wake (a Trefftz plan view) was illuminated by an 800-W xenon arc lamp with a specially designed lens and light slit system. The positions of the dye-marked vortices in this illuminated slice through the wake were photographically recorded.

Experimental Procedure

It has been concluded that the scaling laws for modeling fluid phenomena, pertinent to the study of wake vortices, are essentially the same for tests in water as in air[9] and that the forces acting on hydrofoils operated at depths greater than two chord lengths are essentially unaffected by the free surface and are equal to those obtained on a wing operating in an infinite medium.[10] The model centerline in these tests was located approximately five chord lengths (0.75 of a span) below the free surface. The test Reynolds number (1.64×10^5 based on chord) was considerably less than full scale. However, since agreement in wake appearance was evident where comparisons could be made with flight photographs,[2] the wake interaction data obtained in this test should be indicative of flight results. This seemingly lack of Reynolds number sensitivity does not come as a complete surprise, since previous wake-vortex velocity measurements obtained in this facility[3] on a variety of wing configurations correlated[11] well with both wind-tunnel and flight measurements.

Cameras were operated at constant frame speeds, allowing vortex age to be determined from the photographic records and knowledge of the model towing speed. Immediately after each test run, the carriage was returned to the starting end of the tank for a 15- to 30-min wait for water motion to settle before the next run.

Data Acquisition and Presentation

Typical 35-mm photographic data showing a cross section of the wake as it appears in the light sheet are presented in Fig. 5. This type of photographic information provides a qualitative understanding of the interactions of vortices in multiple-vortex wakes. In addition, changes in vortex positions as the wake aged were obtained from the

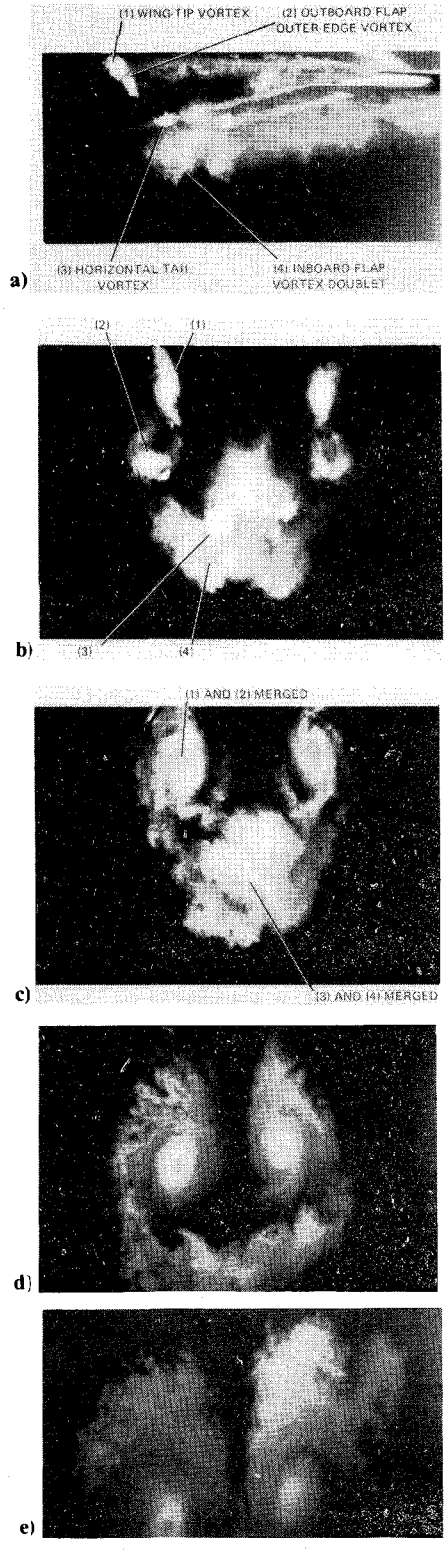

Fig. 5 Cross section of wake in light sheet – LDG configuration, $\alpha = 2.9$ deg, $U_\infty = 1$ m/sec: a) $X/b = 1.3$, b) $X/b = 2.6$, c) $X/b = 6.6$, d) $X/b = 19.7$, e) $X/b = 41$.

photographs by correcting for both camera viewing and cone angles. Vortex trajectories and trajectory parameters thus obtained are presented and discussed in subsequent figures.

Effect of Wingspan Loading on Wake

Landing Configuration

The wingspan load distribution determines the number, strength, and location of vortices in the wake of the wing. The isolated vortex shed from each side of an elliptically loaded

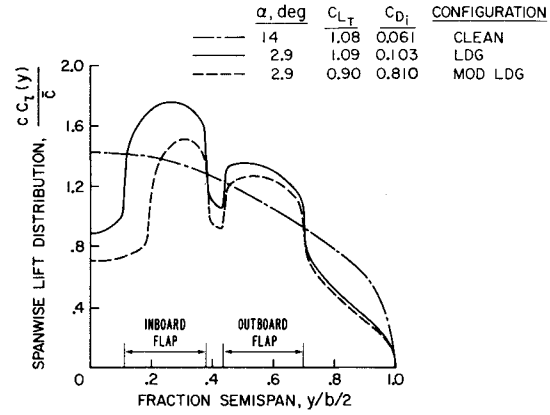

Fig. 6 Predicted spanwise lift distribution; CLEAN, LDG, and MOD LDG configurations.

swept wing is a result of the load gradient at the wing tips (Fig. 6). The landing configuration of the 747 (LDG) consists of all flaps deflected trailing edges down 46° (Fig. 2). In this configuration, five vortices are shed from each side of the wing (Fig. 5a). This is a result of the multiple span-load gradients caused by the flaps (Fig. 6) – predicted span loadings presented here were calculated using the vortex-lattice method.[12] By a distance of six span lengths behind the LDG configuration, the wingtip vortices move upward and inboard and completely merge with the vortices from the outboard edge of the outboard flaps (Fig. 5a-c). The result is two persistent isolated vortices (Fig. 5d, e). The remaining flap vortices merge with the vortices from the tips of the horizontal stabilizer and form a region of diffused vorticity at and below the aircraft centerline (Fig. 5c).

LDG/O Configuration

A LDG/O configuration consisting of the inboard flaps deflected trailing edges down 46 deg and outboard flaps set at zero deflection was theoretically[2] and experimentally[4-7,13] found to result in an alleviation of the persistent vortices associated with the landing configuration. The predicted span loading is shown in Fig. 7. The vortex associated with the steep gradient in span loading at the outboard edge of the inboard flap is the dominant vortex of the three vortices shed from each side of the wing. Under its influence, the vortex from the inboard side of the flap is rotated to a position directly below it, and the wingtip vortex moves up, inboard, and then down to orbit about and merge with this outboard-edge flap vortex, resulting in a large, diffuse, slowly rotating vortex by 23 span lengths downstream.

However, recent flight tests[6,7] have indicated that, although the LDG/O span loading does alleviate the wake rotational velocities associated with the conventional landing configuration, deployment of the landing gear substantially reduced the benefits of modifying the span loading. As a result, the flow-visualization technique described above was used to examine the far-field wake for differences in vorticity as a consequence of deploying the landing gear.

With gear deployed, the following changes in the wake were noted: a) the vortex doublet from the flap appeared more diffuse; b) the merger of wingtip vortex with outer-edge flap vortex occurred sooner; c) at 23 span lengths downstream, the wake consisted of two diffuse, slowly rotating vortices, but they were less diffuse than for the gear-retracted condition; d) by 40 span lengths, these diffuse vortices began to contract and reform once again into smaller, more concentrated areas of vorticity. A near-field comparison of wingtip vortex trajectories for the LDG/O configuration at a 5.8 deg angle of attack with and without landing gear is presented in Figs. 8 and 9. These data were obtained from the photographic records. Figure 8 presents the distance between the wingtip vortices as a function of downstream distance. These vortices

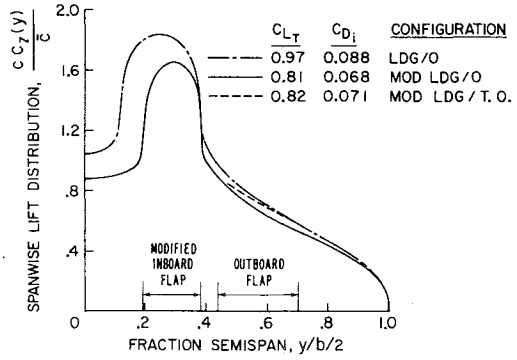

Fig. 7 Predicted spanwise lift distribution; LDG/O, MOD LDG/O, and MOD LDG/T.O. configurations; $\alpha = 5.8$ deg.

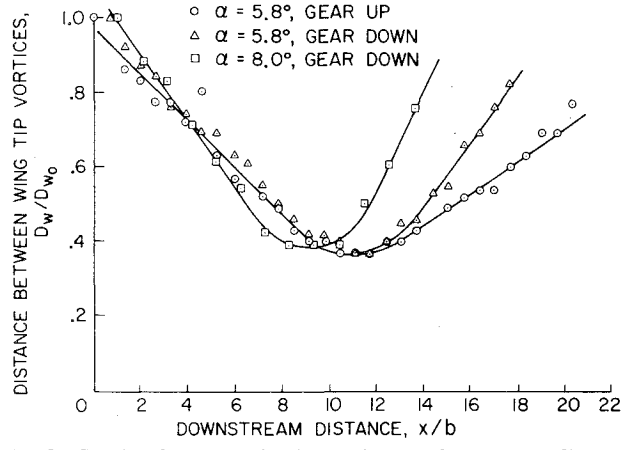

Fig. 8 Spacing between wingtip vortices vs downstream distance; LDG/O configuration.

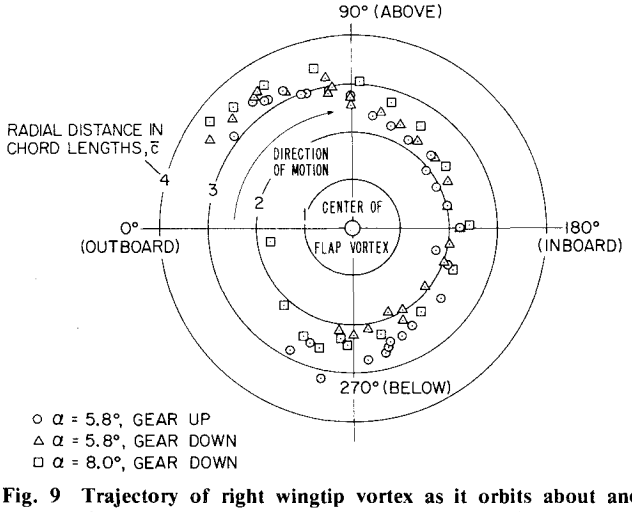

Fig. 9 Trajectory of right wingtip vortex as it orbits about and merges with the vortex shed from the outboard edge of the right inboard flap; LDG/O configuration.

move inboard in a spiral trajectory about the flap outer-edge vortex. The distance between them decreases and reaches a minimum when they pass directly between the outer-edge flap vortices (~10 span lengths downstream). Their separation distance then begins to increase as they move outboard and merge with the flap vortices at about 17 to 20 span lengths downstream. Up to the time of minimum separation, there are no discernible gear effects; however, as the merging process continues, the tip vortices associated with the gear-down configuration move apart at twice the rate of the gear-up vortices and merge sooner.

Figure 9 shows the spiral trajectory of the right-wingtip vortex as it orbits and merges with the vortex from the outer edge of the right inboard flap. At a 5.8 deg angle of attack, the effect of the landing gear on the trajectory begins to appear in the third quadrant as an acceleration of the inward spiral of the wingtip vortex. This suggests that the presence of the gear may result in preserving concentrated vorticity at the outboard edge of the flap, and is probably associated with a weakening of the inner-edge vortex due to its proximity to the turbulence generated by the gear. Also shown in Figs. 8 and 9 are the wingtip vortex trajectories for the LDG/O configuration at an 8 deg angle of attack with gear deployed. At this higher angle of attack, the tip vortex reaches a greater distance from the flap vortex as it moves up and inboard; but when the tip vortices pass between the flap outer-edge vortices, their minimum separation distance is comparable to the 5.8 deg angle of attack. As the tip vortices rotate through the third quadrant, they – like the low-angle-of-attack gear-down configuration – accelerate their inward spiral to merge with the flap vortex. After merging, the resulting two diffuse vortices eventually reformed into two well-defined vortices again.

When this configuration was tested at an angle of attack of 2.9 deg with the gear up, the flap and tip vortices did not merge and the wingtip vortices persisted. The horizontal tail vortices merged with the outer-edge flap vortices and both were dissipated before the very slow-moving wingtip vortices moved inboard and down. The relative strengths and speeds of the horizontal tail and wing and flap vortices appear to play significant roles in the dynamics of the vortex system.

The effect of horizontal tail incidence was investigated for the LDG/O gear-up configuration. The tail incidence was varied from +4 to −4 deg, without any noticeable changes in the trajectories or merging characteristics of the flap and wingtip vortices. In all cases, the vortex from the tail moved downward and merged with the flap vortices. This descent is associated with both their relatively weak strength (as compared to wing vortices) and the induced downward component of velocity in their flowfield created by the rotational velocities of the flap vortices.

Recent flight tests[6,7] of a Boeing 747 in the LDG/O (gear-up) configuration have indicated that the effect of 5 deg yaw on the wake reduces the vortex alleviation of the leeward vortex. As a result of this conclusion, the water tank model was tested in the LDG/O configuration with 5 deg yaw at an angle of attack of 5.8 deg. No obvious asymmetries due to yaw were noticed in the wake. Perhaps the asymmetries in flight resulted from control deflections required to maintain level flight.

Modified Flap Configurations

In an attempt to eliminate the gear effect on the wake alleviation capability of the LDG/O configuration, 30% of the inboard span of the flap was removed. This configuration was designated MOD LDG/O. The purpose was to move the inboard flap vortex pair closer together. The result would be a rotation of the flap inboard edge vortex away from the region of the fuselage and turbulence associated with the landing gear. The predicted span-load distribution for this configuration at a 5.8 deg angle of attack is shown in Fig. 7. The load gradient at the inboard side of the flap has been steepened, suggesting that the net result on the flap vortex pair might be to swing down and out as the inboard vortex rotates below the outboard vortex.

The flow visualization indicated an inner-edge flap vortex much less diffuse than it was in the LDG/O configuration, and that immediately after formation it began to rotate below the outer-edge flap vortex. At about two span lengths downstream, the tail vortex began to merge with the flap outer-edge vortex; two span lengths later they were completely merged and the inner-edge vortex was directly below the outer-edge vortex. An elongation of the flap doublet resulted

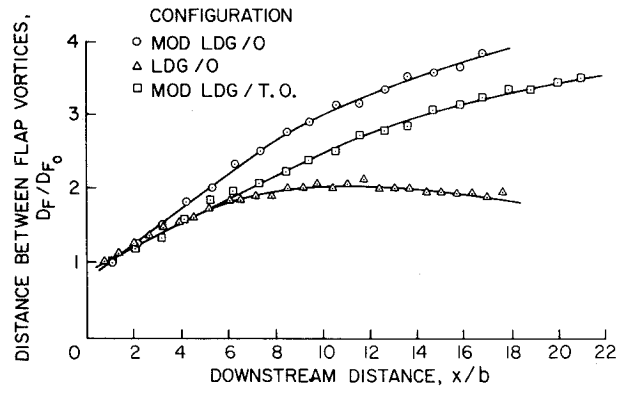

Fig. 10 Spacing between vortices shed from the outboard edge of the inboard flaps vs downstream distance; $\alpha = 5.8$ deg, gear down.

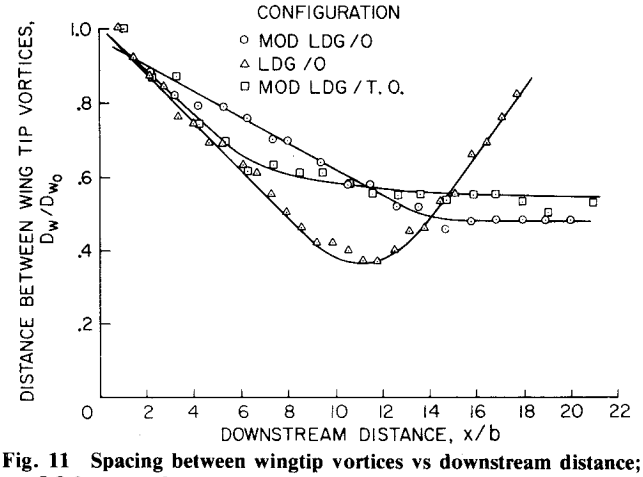

Fig. 11 Spacing between wingtip vortices vs downstream distance; $\alpha = 5.8$ deg, gear down.

from the tail merging. The vortices from the outboard edge of the inboard flap began to drift down and outboard immediately after formation. Figure 10 compares their separation distance as a function of downstream distance. Both the MOD LDG/O and LDG/O results are shown. The outer-edge flap vortex moves outboard at a greater rate and to a greater distance for the modified configuration. As the flap doublets moved apart, their vortices became more diffuse and elongated. By 16 span lengths, when the wingtip vortices were passing between the flap doublets, it was no longer possible to identify individual flap vortices.

The wingtip vortices moved up and inboard and then down between the flap doublets. They never merged with the outward-moving, diffuse, flap vortices. Figure 11 compares the separation distance between the wingtip vortices as a function of downstream distance for the MOD LDG/O and LDG/O configurations. The tip vortices move together at a slower rate for the modified configuration, and after 180 deg of rotation about the outer-edge flap vortices (at about 16 span lengths downstream) they remain at a constant distance from each other as they persist and slowly descend. A comparison of trajectories of the right wingtip vortex about the right outer-edge flap vortex for the MOD LDG/O and LDG/O configurations is presented in Fig. 12.

In an attempt to slow the outboard movement of the flap doublet – in anticipation of a resulting flap, wingtip, vortex interaction – the outboard flaps were lowered to the takeoff position. This configuration was called the MOD LDG/T.O. The predicted span loading at a 5.8 deg angle of attack is presented in Fig. 7. The outboard-edge vortex from the inboard flap was more diffuse, and the outboard-edge vortex from the outboard flap merged with the wingtip vortex at about three span lengths. This merging of the flap vortex with

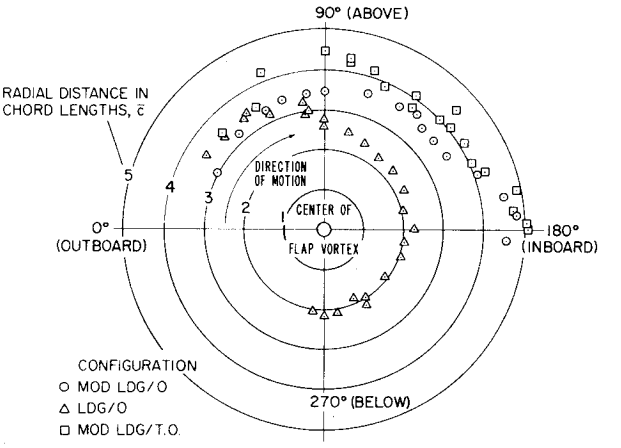

Fig. 12 Trajectory of right wingtip vortex as it orbits about and merges with the vortex shed from the outboard edge of the right inboard flap; $\alpha = 5.8$ deg, gear down.

the wingtip vortex caused the latter to elongate in cross section and induce a spiral arm in the shape of the tip vortex.

The movement outboard of the inboard flap's vortex doublet was slowed by deployment of the outboard flaps to the takeoff position. This is evident in Fig. 10. Although these flap vortices stayed closer to the model centerline than the MOD LDG/O configuration, they were still far enough apart to allow the wingtip vortices to pass between them without merging. The wingtip vortex trajectories for this configuration are shown in Figs. 11 and 12. Figure 12 suggests that for the modified configuration, after 90 deg of rotation of the wingtip vortex about the flap vortex, the trajectory of the wingtip vortex is primarily influenced by its proximity to the wingtip vortex from the other side of the wing.

Since the change from the MOD LDG/O to the MOD LDG/T.O. configuration slowed the outboard movement of the inboard flap doublet – although not enough to cause flap wingtip vortex merging – the decision was made to lower the outboard flaps still farther to the landing position. This was called the MOD LDG configuration. Its predicted span loading at a 2.9 deg angle of attack is presented in Fig. 6. The wake characteristics resembled those of the landing configuration in the near field, but did not appear to develop into the persistent vortices associated with the landing configuration in the far field (Fig. 13). The wake had none of the characteristics of the other modified configurations.

The outboard-edge vortex off the inboard flap rotated very rapidly to a position directly below the inboard-edge vortex and the doublet moved inward toward the model centerline (Figs. 13a-c) when at 2.6 span lengths it merged with the doublet from the opposite side. The merging resulted in a diffuse cloud with no distinguishable vortices remaining (Figs. 13c, d). The horizontal tail vortices moved down but were outboard of the merged flap doublets and did not merge with them (Fig. 13). The wingtip vortices moved up and inboard, and at 6.5 span lengths merged with the vortices from the outboard side of the outboard flaps (Fig. 13d). These merged vortices were dominated by the flap vortices and appeared to grow in diameter and merged with the tail vortices at 13 span lengths (Fig. 13e.) The resulting vortices descended at 1/3 the rate of those of the landing configuration and drifted outboard from each other (Figs. 14 and 15). As they drifted down and outward, they became increasingly diffuse and after 30 span lengths downstream appeared as separate, slowly rotating areas of large dye clouds (Fig. 13g). The far wake of this configuration appeared to contain the least visible amount of concentrated vorticity and suggests a possible alleviation scheme.

Since removing 30% of the inboard side of the inboard flap of the landing configuration results in a 0.19 reduction in lift coefficient (at an angle of attack of 2.9 deg). MOD LDG

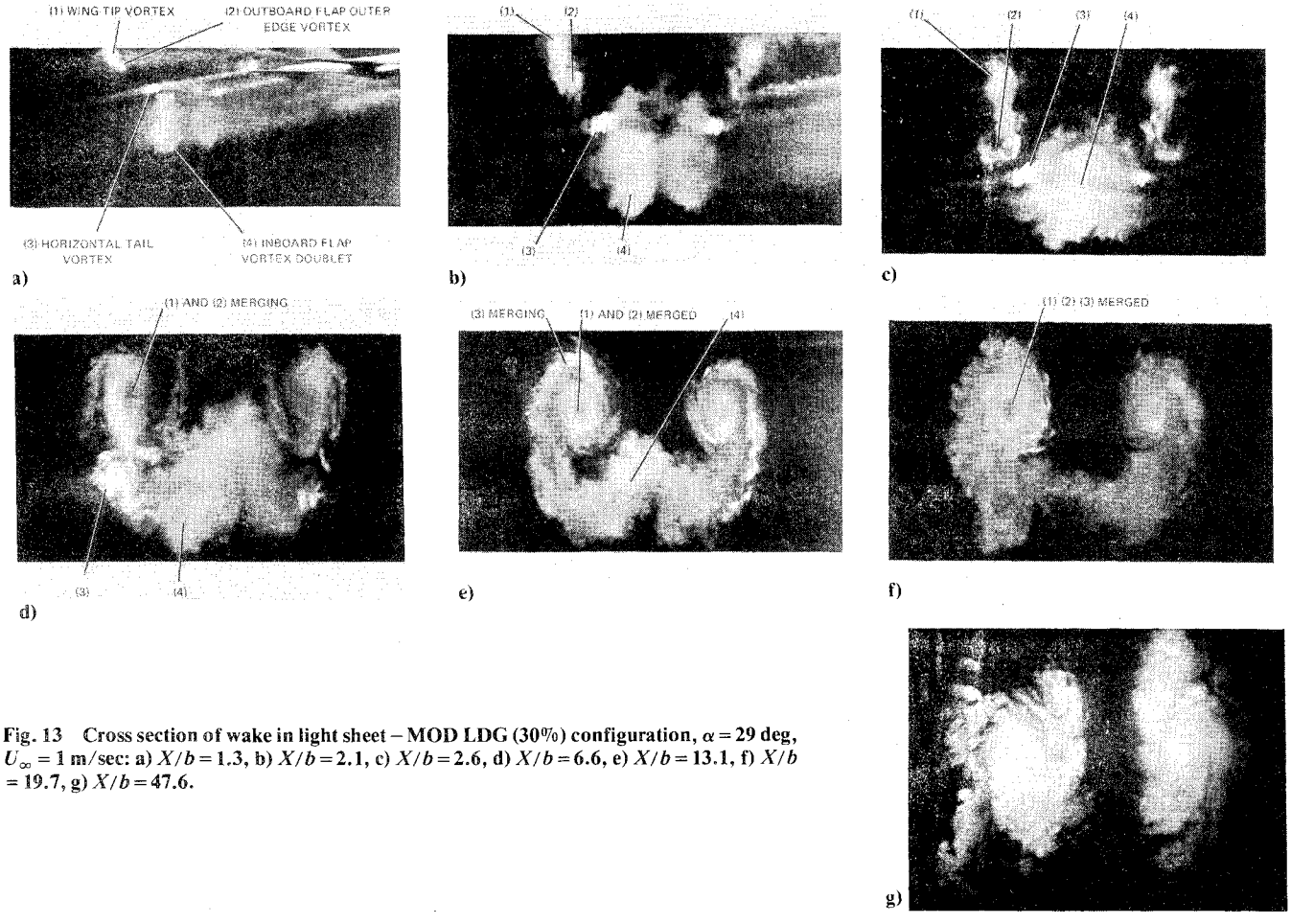

Fig. 13 Cross section of wake in light sheet – MOD LDG (30%) configuration, $\alpha = 29$ deg, $U_\infty = 1$ m/sec: a) $X/b = 1.3$, b) $X/b = 2.1$, c) $X/b = 2.6$, d) $X/b = 6.6$, e) $X/b = 13.1$, f) $X/b = 19.7$, g) $X/b = 47.6$.

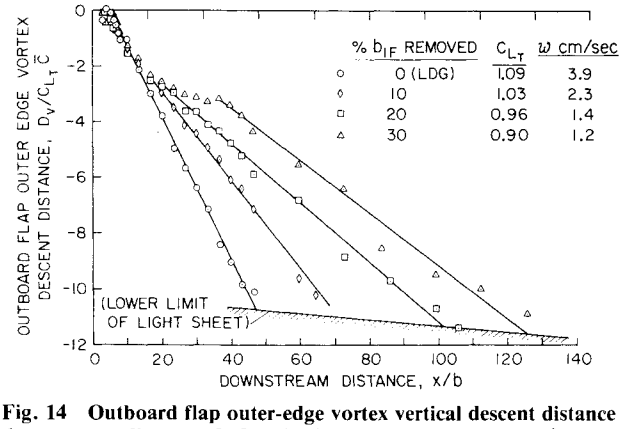

Fig. 14 Outboard flap outer-edge vortex vertical descent distance vs downstream distance, MOD LDG configurations, $\alpha = 2.9°$, $U_\infty = 1$ m/sec.

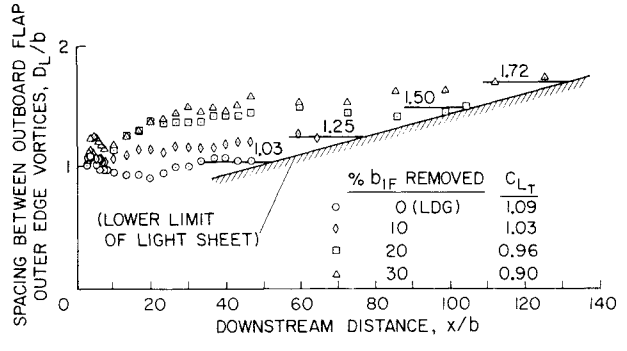

Fig. 15 Spacing between outboard flap outer-edge vortices vs downstream distance, MOD LDG configurations, $\alpha = 2.9°$, $U_\infty = 1$ m/sec.

configurations with 10 and 20% of the flap removed were also investigated. These results are also presented in Figs. 14 and 15. The wakes of the 20% MOD LDG and 30% MOD LDG configurations resembled each other, and the wakes of the 10% MOD LDG and the LDG configurations were similar. The slopes of the lines faired through the data in Fig. 14 are the sink rates, w, of the remaining outboard flap outer-edge vortices. Within the scatter of the data, the sink rates remain constant (linear slope), while the vortices were visible in the light sheets. As the inboard flap span is reduced, the vortex sink rate is reduced. The figure also indicates that as the span of the inboard flap is reduced, the resulting wake takes longer to complete the merging process and achieve a final rolled-up state and constant sink rate. The lower limit of the light sheet was approximately 3/4 of a span from the bottom of the tank. Calculations of tank free surface and boundary effects on the trajectories of these vortices traversing the middle third section of the tank (illuminated by the light sheet) were found to be negligible.

The downward velocity (or sink rate) of a vortex pair is proportional to total lift coefficient and inversely proportional to the vortex spacing squared. The ordinate in Fig. 14 was normalized by the total lift coefficient, hence differences in sink rates are a result of differences in vortex spacing. Asymptotic values of the measured separation distance of the vortices as they leave the light sheet are indicated in Fig. 15. Configurations with the lowest sink rates are seen to have the greatest vortex spacing. Using these results, the comparison shown in Table 2 was made. The agreement is seen to be good.

Table 2 Comparison of measured vortex sink rates and spacings

Configuration	$\frac{(w/C_L)_{LDG}}{(w/C_L)_{MOD\,LDG}}$ (from Fig. 14)	$\left(\frac{b_{e_{MOD\,LDG}}}{b_{e_{LDG}}}\right)^2$ (from Fig. 15)
10% MOD LDG	1.6	1.5
20% MOD LDG	2.5	2.1
30% MOD LDG	2.7	2.7

The fact that the final two vortices for the MOD LDG configurations are located outboard of the wing tips is also consistent with the predicted spanload distributions for these configurations (Fig. 6). It can be shown from conservation of vorticity and first moment of vorticity that

$$D_L/b = C_L/[cC_{l(0)}/\bar{c}]$$

in the far field. This ratio is greater than 1 for the MOD LDG configuration and increases with decreasing inboard flap span. This basic conclusion was not affected by inaccuracies in the vortex lattice method resulting from failure to include fuselage or tail lift contributions.

If vortex descent distance for the LDG configuration at 49 span lengths (Fig. 14) is converted to distance below a full-scale Boeing 747, the trailing vortices at 1.2 km behind the generating aircraft are 113 m below it. This result is consistent with the measurements behind a C-5A.[14]

An attempt was made to simulate the 30% MOD LDG configuration by placing a wedge spoiler in front of the inboard 30% of the inboard flap. The wedge angle was 45%. The near-field wake (to about 30 span lengths) resembled the 20% MOD LDG configuration, but the wake was much more turbulent in appearance. The vortex sink rate and spacing in the far field were between those of the 10 and 20% MOD LDG configurations.

Conclusions

A flow visualization technique has been developed and used to investigate vortex interactions in multiple vortex wakes. Different wake characteristics were generated by changing both the attitude and flap geometry of a 0.01-scale model of a Boeing-747 transport. The following results were obtained:

1) The behavior of these wakes can be sensitive to small changes in wingspan loading or model attitude. Realistic span loadings were achieved which caused multiple vortex interactions and merging within the wake, resulting in diffuse, slowly rotating wakes. Removing the inboard 30% of the span of the inboard flaps of the landing configuration changed the wake from being characterized by two persistent, highly concentrated vortices to a wake with dispersed vorticity by 30 span lengths downstream. Changes in model angle of attack for a given configuration showed that both the relative strengths and path speeds of the vortices in a multiple-vortex wake play important roles in characterizing the final wake.

2) It was observed that landing-gear deployment caused a far-field reconcentration of vorticity behind the LDG/O model configuration. This is in agreement with results of recent flight tests of the Boeing 747 reporting that LDG/O gear deployment causes reduction of vortex alleviation.

3) Generally, vortices that remain isolated in a multiple vortex wake – in the absence of external disturbances – tend to persist. Alleviation of wake vorticity is attained by causing the wake vortices to interact and merge.

4) The vortices shed from the horizontal stabilizer always moved down into the wake and merged with other vortices – primarily the inboard flap vortices. Although the tail developed negative lift for most of the configurations tested, the local induced-velocity field forced its wake downward. When they merged with the flap vortices, distortions or elongations were usually caused in the dye pattern of the flap vortices. The tail vortices seem to play a significant role in vortex interactions within the wake; however, their ultimate effect on the wake must be ascertained quantitatively.

5) When the model was yawed 5 deg with its inboard flaps in the landing position and outboard flaps retracted, there were no obvious asymmetries visible in the wake. The effects of yaw seen in flight may have resulted from control deflections required to maintain flight attitude equilibrium.

6) The water tow facility has proved to be an extremely useful tool in investigating the wake characteristics behind aircraft models, particularly in the far field, a region of interest that cannot be explored in wind tunnels. Far-field wake characteristics suggested from flight tests[6] have been verified in the water tow facility.

References

[1]Betz, A., "Behavior of Vortex Systems," NACA TM 713, June 1933.

[2]Anon., "NASA Symposium on Wake Vortex Minimization," NASA SP-409, 1976.

[3]Ciffone, D. L. and Orloff, K. L., "Far-Field Wake-Vortex Characteristics of Wings," *Journal of Aircraft*, Vol. 12, May 1975, pp. 464-470.

[4]Corsiglia, V. R., Rossow, V. J., and Ciffone, D. L., "Experimental Study of the Effect of Span Loading on Aircraft Wakes," NASA TM X-62, 431, May 1975.

[5]Dunham, E. R., Jr., "Model Tests of Various Vortex Dissipation Techniques in a Water Towing Tank," NASA TN (to be published).

[6]Tymczyszyn, J. and Barber, M. R., "A Review of Recent Wake Vortex Flight Tests," 18th Annual Symposium of Society of Experimental Test Pilots, Los Angeles, Calif., Sept. 26, 1974.

[7]Smith, H. J., "A Flight Test Investigation of the Rolling Moments Induced on a T-37B Airplane in the Wake of a B-747 Airplane," NASA TM X-56, 031, April 1975.

[8]Orloff, L. L., Ciffone, D. L., and Lorincz, D., "Airfoil Wake Vortex Characteristics in the Far Field," NASA TM X-62,318, Nov. 1973.

[9]Kirkman, K. L., Brown, C. E., and Goodman, A., "Evaluation of Effectiveness of Various Devices for Attenuation of Trailing Vortices Based on Model Test in a Large Towing Basin," NASA CR-2202, Dec. 1973.

[10]Wadlin, K. L., Ramsen, J. A., and McGehee, J. R., "Tank Tests at Subcavitation Speeds of an Aspect Ratio 10 Hydrofoil with a Single Strut," NACA RM L9K14a, July 1950.

[11]Iversen, J. D., "Correlation of Turbulent Trailing Vortex Decay Data," *Journal of Aircraft*, Vol. 13, May 1976, pp. 338-342.

[12]Hough, G., "Remarks on Vortex-Lattice Methods," *Journal of Aircraft*, Vol. 10, May 1973, pp. 314-317.

[13]Ciffone, D. L. and Lonzo, C., Jr., "Flow Visualization of Vortex Interactions in Multiple Vortex Wakes Behind Aircraft," NASA TM X-62,459, June 1975.

[14]Andrews, W. H., Robinson, G. H., and Larson, R. R., "Exploratory Flight Investigation of Aircraft Response to the Wing Vortex Wake Generated by Jet Transport Aircraft," NASA TN D-6655, March 1972.